Short Article

Cell Host & Microbe

The *Chlamydia trachomatis* Inclusion Membrane Protein CpoS Counteracts STING-Mediated Cellular Surveillance and Suicide Programs

Graphical Abstract

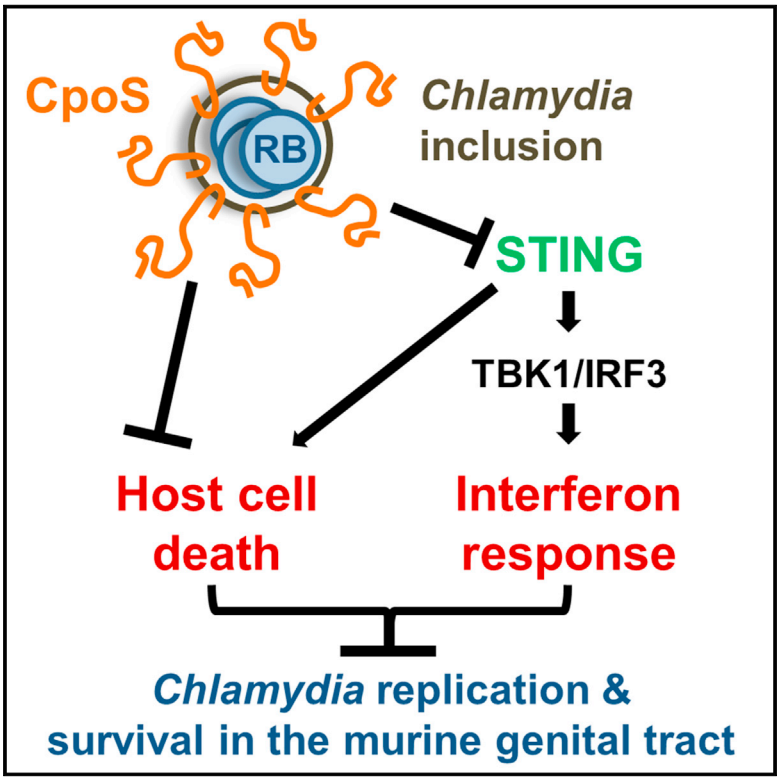

Highlights

- A genetic screen identifies *C. trachomatis* effector CpoS as a regulator of cell death
- Loss of CpoS on the inclusion causes enhanced death in infected cells
- DNA sensor STING modulates IFN responses and death in cells infected with *cpoS* mutants
- *cpoS* mutants are defective for propagation in cell culture and in mice

Authors

Barbara S. Sixt, Robert J. Bastidas, Ryan Finethy, ..., Guido Kroemer, Jörn Coers, Raphael H. Valdivia

Correspondence

raphael.valdivia@duke.edu

In Brief

Evading cell death is critical for *Chlamydia trachomatis* to maintain a replicative niche. Sixt et al. show that the *Chlamydia* effector protein CpoS counteracts STING-mediated pro-death signals and type I IFN responses in response to *Chlamydia*-containing vacuoles, which enables optimal intracellular bacterial growth and survival in the murine genital tract.

Sixt et al., 2017, Cell Host & Microbe *21*, 113–121
January 11, 2017
http://dx.doi.org/10.1016/j.chom.2016.12.002

CellPress

Cell Host & Microbe
Short Article

The *Chlamydia trachomatis* Inclusion Membrane Protein CpoS Counteracts STING-Mediated Cellular Surveillance and Suicide Programs

Barbara S. Sixt,[1,2,3,4,5] Robert J. Bastidas,[1] Ryan Finethy,[1] Ryan M. Baxter,[1] Victoria K. Carpenter,[1] Guido Kroemer,[2,3,4,5,6,7] Jörn Coers,[1,8] and Raphael H. Valdivia[1,9,*]
[1]Department of Molecular Genetics and Microbiology, Duke University, Durham, NC 27710, USA
[2]INSERM U1138, Centre de Recherche des Cordeliers, Paris 75006, France
[3]Equipe 11 labellisée Ligue Nationale contre le Cancer, Centre de Recherche des Cordeliers, Paris 75006, France
[4]Université Paris Descartes, Paris 75006, France
[5]Metabolomics and Cell Biology Platforms, Institut Gustave Roussy, Villejuif 94800, France
[6]Pôle de Biologie, Hôpital Européen Georges-Pompidou, AP-HP, Paris 75015, France
[7]Karolinska Institute, Department of Women's and Children's Health, Karolinska University Hospital, Stockholm 17176, Sweden
[8]Department of Immunology, Duke University, Durham, NC 27710, USA
[9]Lead Contact
*Correspondence: raphael.valdivia@duke.edu
http://dx.doi.org/10.1016/j.chom.2016.12.002

SUMMARY

Evading cell death is critical for *Chlamydia* to maintain a replicative niche, but the underlying mechanisms are unknown. We screened a library of *Chlamydia* mutants for modulators of cell death. Inactivation of the inclusion membrane protein CpoS (*Chlamydia* promoter of survival) induced rapid apoptotic and necrotic death in infected cells. The protection afforded by CpoS is limited to the inclusion in which it resides, indicating that it counteracts a spatially restricted pro-death signal. CpoS-deficient *Chlamydia* induced an exacerbated type I interferon response that required the host cGAS/STING/TBK1/IRF3 signaling pathway. Disruption of STING, but not cGAS or IRF3, attenuated cell death, suggesting that STING mediates *Chlamydia*-induced cell death independent of its role in regulating interferon responses. CpoS-deficient strains are attenuated in their ability to propagate in cell culture and are cleared faster from the murine genital tract, highlighting the importance of CpoS for *Chlamydia* pathogenesis.

INTRODUCTION

The success of intracellular pathogens depends on their ability to evade cell-autonomous defense responses (Randow et al., 2013). For instance, the induction of host cell death can deprive pathogens from a replicative niche (Labbé and Saleh, 2008). This response is especially effective against obligate intracellular pathogens such as the sexually transmitted *Chlamydia trachomatis*, which is associated with pelvic inflammatory disease and infertility (Mylonas, 2012). *Chlamydia* spp. alternate between two developmental stages: the non-infectious reticulate body (RB) that replicates within a membrane-bound vacuole (termed inclusion) and the environmentally resistant elementary body (EB) (Ward, 1988). Because the developmental cycle needs to be complete to generate infectious EBs, maintenance of host cell viability during the RB replication phase is critical for the propagation of *Chlamydia* spp. Candidate *Chlamydia* effectors that may protect the inclusion include a family of integral inclusion membrane proteins (Incs) (Rockey et al., 2002). In this study, we employed emerging genetic tools in *Chlamydia* to identify and characterize a *C. trachomatis* mutant lacking the Inc CpoS. Infection with this mutant resulted in premature death of the host cell, hyper-induction of type I interferons, decreased production of EBs, and rapid clearance from the murine genital tract.

RESULTS

A Genetic Screen Identifies a *C. trachomatis* Mutant with Enhanced Cytotoxicity

We screened *C. trachomatis* mutants (Kokes et al., 2015) for strains that induce cytotoxicity in cervical epithelial (HeLa) and monocytic (THP-1) cells at mid-stage of infection. We identified mutant strains that caused the release of higher levels of host lactate dehydrogenase (LDH) as compared to the parent strain CTL2-R (Figure 1A) and focused our analysis on mutant CTL2-M007, which reproducibly induced enhanced LDH release (Figure S1A) and host cell permeability to propidium iodide (Figure 1B). In HeLa cells, death was first detectable at 18 hpi (Figure 1C). The magnitude of the response was dependent on the bacterial dose (Figure S1B) and cytotoxicity required bacterial viability and de novo protein synthesis (Figure S1C). Infections with purified EBs caused levels of cell death similar to those seen in infections with crude bacterial preparations (Figure S1D), indicating that death was not induced by soluble factors.

CTL2-M007-Infected Cells Display Features of Apoptotic and Necrotic Cell Death

CTL2-M007-induced death was also observed in differentiated THP-1 cells, A2EN (human endocervical epithelial) cells,

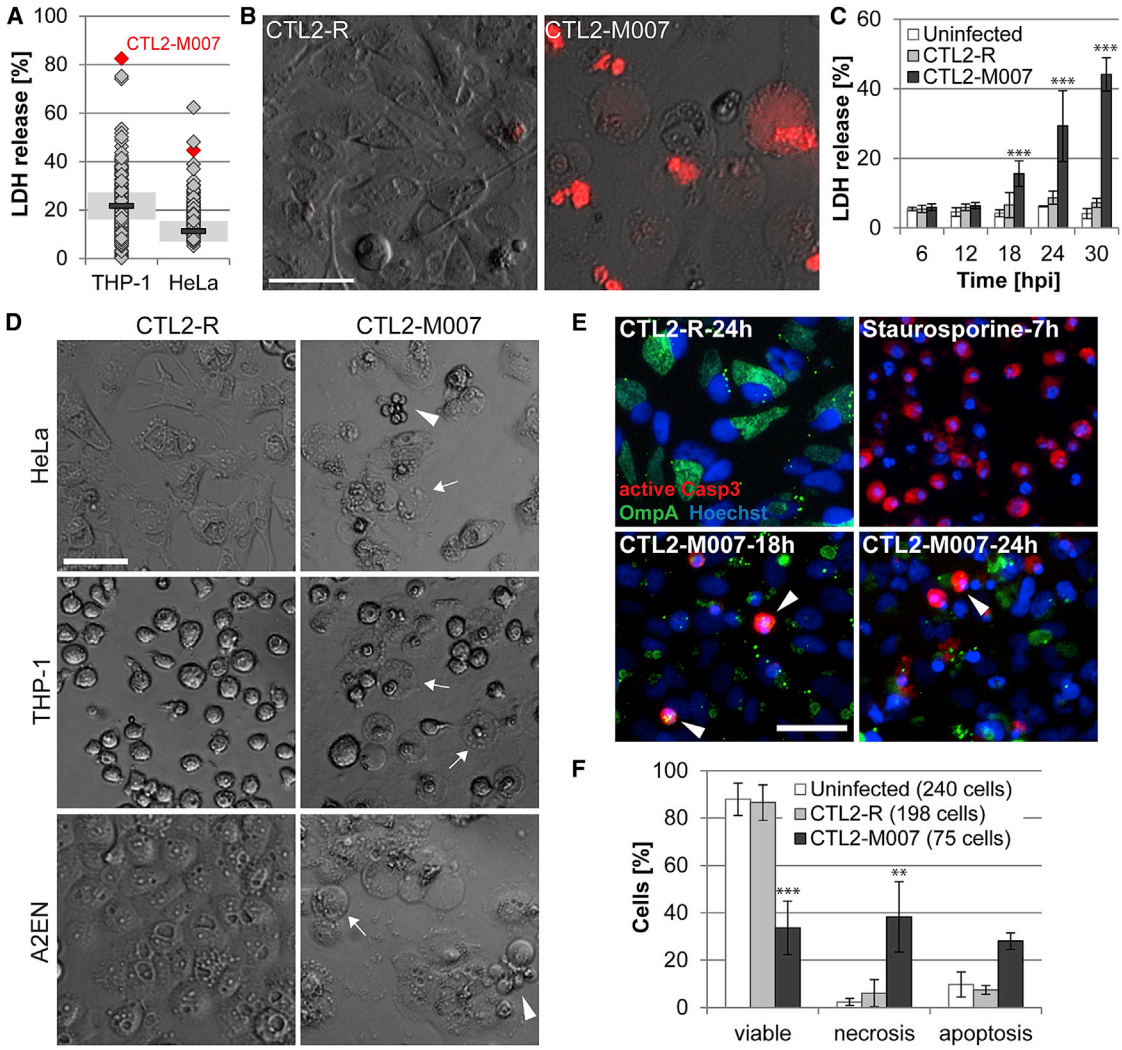

Figure 1. A Genetic Screen Identifies a *C. trachomatis* Strain that Causes Apoptotic and Necrotic Cell Death

(A) Cell lysis induced by *Chlamydia* mutants as assessed by the release of LDH into supernatants at 28 hpi (THP-1) or 24 hpi (HeLa) (mutants [diamonds, n = 224]; CTL2-R [bar, mean; shaded area, SD; n = 2]).

(B) Loss of membrane integrity during infection of HeLa cells with CTL2-M007 (10 IFU/cell) visualized by enhanced permeability to propidium iodide (red) at 24 hpi (scale bar, 50 μm).

(C) Time course of cell death induction by CTL2-M007 (10 IFU/cell) in HeLa cells (mean ± SD, n = 3, two-way ANOVA + Newman-Keuls).

(D) Induction of apoptosis (arrowheads) and necrosis (arrows) by CTL2-M007 in epithelial (HeLa, A2EN) and monocytic (THP-1) cells (10 IFU/cell, 21 hpi). Scale bar, 50 μm.

(E) Immunofluorescence detection of apoptotic CTL2-M007-infected (10 IFU/cell) HeLa cells (*Chlamydia* OmpA, green; active caspase-3, red; Hoechst, blue). Arrowheads indicate apoptotic infected cells. Scale bar, 50 μm.

(F) Live-imaging-based assessment of the frequency of apoptosis and necrosis in CTL2-M007-infected (10 IFU/cell) cells until 30 hpi. The category "uninfected" refers to inclusion-free cells in infected wells (mean ± SD, n = 2, two-way ANOVA + Newman-Keuls).

See also Figure S1 and Movies S1–S3.

HEK293T (human embryonic kidney) cells, and MEFs (mouse embryonic fibroblasts) (Figures 1D and S1E) but was less pronounced in Vero cells (Figure S1F). THP-1 cells died by a necrotic-type of death generating balloon-like cell remnants (Figures 1D and S1E). In non-phagocytic cells, a proportion of cells adopted an apoptosis-like morphology characterized by cell shrinkage, rounding, and membrane blebbing (Figures 1D and S1E). Indeed, CTL2-M007-infected HeLa cells displayed hallmarks of caspase-dependent apoptosis, including condensed nuclei, immunoreactivity to antibodies specific for proteolytically mature caspase-3 (Figure 1E), and caspase-3 activity based on the cleavage of the fluorescent substrate NucView-488 (Figure S1G) and DEVD cleavage activity in cell lysates (Figure S1H). These features were similar to those induced by the apoptosis inducer staurosporine (Figures 1E and S1H). Time-lapse microscopy indicated that by 30 hpi only 34% of the HeLa cells infected with CTL2-M007 remained viable, 28% had died with features of apoptosis, and 38% had disintegrated by necrosis

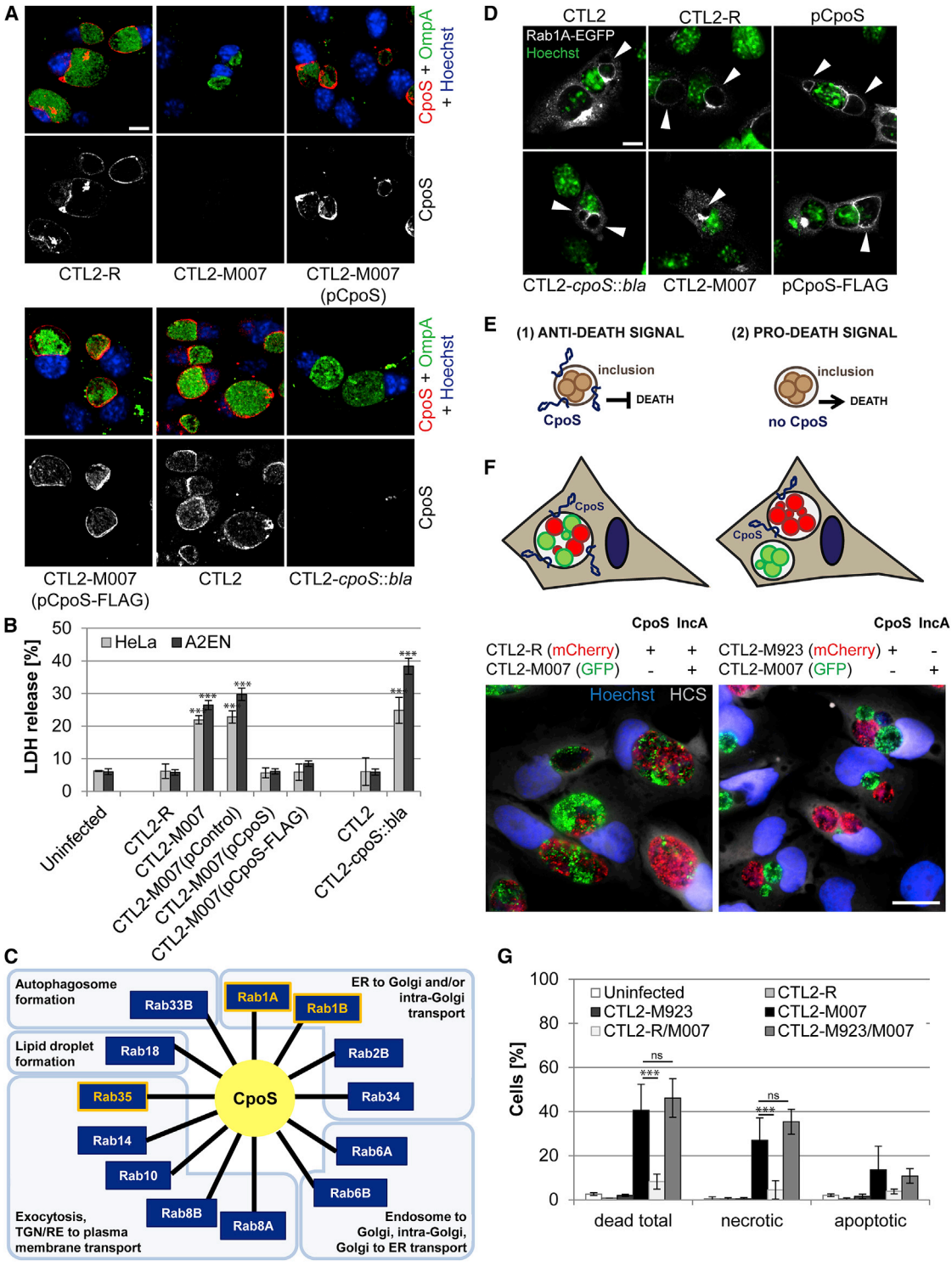

Figure 2. Loss of CpoS on the Inclusion Causes Enhanced Death in Infected Cells

(A) Immunolocalization of CpoS in HeLa cells infected for 26 hr with the indicated *Chlamydia* strains (CpoS, red; OmpA, green; Hoechst, blue; confocal images; scale bar, 10 μm).

(B) Expression of *cpoS* from a plasmid vector rescues the cytotoxicity of CTL2-M007, while targeted disruption of *cpoS* induces host cell death in infected cells. Displayed is extracellular LDH activity (10 IFU/cell, 26 hpi).

(C) Functional diversity of Rab GTPases (Hutagalung and Novick, 2011) that co-immunoprecipitate with CpoS.

(legend continued on next page)

(Figure 1F; Movies S1–S3). In sharp contrast, 88% of inclusion-free cells and 87% of cells containing CTL2-R inclusions remained viable during the same time frame.

CTL2-M007-Induced Cytotoxicity Is Associated with the Loss of the Inc CpoS

CTL2-M007 contains 14 mutations (Table S1). We generated recombinants between CTL2-M007 and wild-type bacteria and mapped the mutation responsible for cytotoxicity to a premature stop codon (Q31*) in the gene CTL0481 (CT229 in *C. trachomatis* serovar D) (Table S2). This gene encodes an Inc protein we refer to as CpoS, for *C*hlamydia *p*romoter *o*f *s*urvival. We next transformed CTL2-M007 with a plasmid enabling expression of full-length *cpoS*. In parallel, we disrupted *cpoS* in CTL2 by insertional gene inactivation with an intron carrying a β-lactamase resistance (*bla*) cassette (Figures S2A and S2B). CpoS was detectable as a 19 kD protein in HeLa cells infected with parental strains, but not CTL2-M007 or CTL2-*cpoS*::*bla* (Figure S2C). CpoS expression was significantly increased in cells infected with the complemented mutant (Figure S2D), and immunofluorescence microscopy indicated that CpoS, as previously shown (Bannantine et al., 2000; Rzomp et al., 2006), localized to the inclusion membrane (Figure 2A). The cytotoxicity induced by CTL2-M007 was abolished by introduction of the CpoS-expressing plasmid (Figure 2B). Disruption of *cpoS* in wild-type bacteria recapitulated the toxicity phenotype observed in CTL2-M007 (Figure 2B). Overall, these findings provide genetic confirmation that the loss of CpoS induces toxicity in infected cells.

We next identified CpoS-interacting proteins by expressing a FLAG-tagged CpoS in CTL2-M007, followed by non-denaturing co-immunoprecipitation with anti-FLAG antibodies and protein identification by mass spectrometry (Figure S2E). Interacting proteins included the Inc protein CTL0476 (CT223 in *C. trachomatis* serovar D), consistent with predictions made by bacterial two-hybrid screens (Gauliard et al., 2015), and multiple Rab GTPases, including previously reported interactions with Rab1A/B and Rab35 (Mirrashidi et al., 2015) (Figure 2C; Table S3), suggesting that CpoS may modulate membrane trafficking. CpoS is necessary for the recruitment of a subset of these Rab proteins, as Rab1A-EGFP did not associate with inclusions in cells infected with *cpoS* mutants (Figure 2D).

Inclusions Lacking CpoS Initiate the Onset of a Death Signal

We considered two scenarios to account for the induction of death in the absence of CpoS: (1) CpoS globally inhibits pro-death signals activated by the presence of inclusions, and (2) the presence of inclusions lacking CpoS initiates a pro-death signal (Figure 2E). To test these scenarios, we took advantage of the fusogenicity of inclusions, a process that requires the protein IncA (Hackstadt et al., 1999). Time-lapse microscopy revealed that inclusions made by CTL2-M007 expressing GFP and CTL2-R expressing mCherry readily fused (Figure 2F; Movie S4) and that the proportion of cells that died was significantly reduced compared to infection with CTL2-M007 alone (Figure 2G). In contrast, inclusions made by the *incA* mutant strain CTL2-M923 (Kokes et al., 2015) (Table S1) failed to fuse with CTL2-M007 inclusions (Figure 2F; Movie S5) and to protect co-infected cells (Figure 2G), despite the presence of CpoS on CTL2-M923 inclusions (Figure S2F). These findings demonstrate that CpoS-defective inclusions initiate the onset of a pro-death signal that cannot be inhibited by CpoS on other inclusions. The protection conferred by CpoS is thus inclusion autonomous.

Inhibitors of Programmed Cell Death Fail to Protect Cells Infected with *cpoS* Mutants

We next explored the contribution of programmed cell death pathways to the death induced by CpoS-deficient strains. The pan-caspase inhibitors Q-VD-OPH and Z-VAD-FMK failed to block CTL2-*cpoS*::*bla*-induced cell death (Figure S3A) at concentrations that blocked apoptosis and secondary necrosis induced by staurosporine or TNF-α (Figures S3B and S3C). Moreover, cell death induction occurred normally in mouse lung fibroblasts (MLFs) deficient for the pyroptotic caspases 1 and 11 (Jorgensen et al., 2011) (Figure S3D) and could not be inhibited by two inhibitors of necroptosis, necrostatin-1 and necrosulfamide (Figure S3E). Cell death induction was also resistant to the cathepsin B inhibitor CA-074 methyl ester and the free radical scavenger butylated hydroxyanisole (BHA) (Figure S3F).

cpoS Mutants Induce an Enhanced Interferon Response

We used RNA-Seq to characterize host transcriptional responses to infection with CTL2 or CTL2-*cpoS*::*bla*, because the cell death induced by *cpoS* mutants was reduced by inhibitors of host protein synthesis or transcription (Figures 3A, S4A, and S4B). The transcriptional profile of A2EN cells infected with the mutant was strongly altered by 18 hpi, with the transcription of 400 host genes increasing by greater than 2-fold as compared to CTL2-infected cells (Figure 3B; Table S4). Gene ontology term enrichment analysis (Mi et al., 2016) and functional annotation clustering (Huang et al., 2009) of differentially expressed genes indicated an enrichment of immunity related genes, including 27 genes encoding cytokines such as IFN-I (IFN-β), IFN-III (IFN-λ1-3), and TNF-α (Figure S4C; Table S4). At least 58% of the upregulated genes are known IFN-I/IFN-III-stimulated genes (ISGs) (Table S4). Differential regulation was confirmed by qPCR analysis for selected targets (Figure S4D). Consistent with the expression analysis, CTL2-*cpoS*::*bla* induced enhanced activation of an A2EN reporter cell line

(D) Recruitment of Rab1A-EGFP to the *Chlamydia* inclusion depends on CpoS. HeLa cells were infected (10 IFU/cell), transfected with Rab1A-EGFP (1 hpi), and analyzed at 26 hpi (Rab1A-EGFP, white; Hoechst, green; confocal images; scale bar, 10 μm). Arrowheads indicate inclusions.

(E) Models for the induction of cell death during infection with *cpoS* mutants.

(F) During co-infection of HeLa cells, CTL2-M007 inclusions (green) fuse with CTL2-R inclusions (red, left panel), but not with CTL2-M923 inclusions (red, right panel). Cells were fixed and stained (Hoechst, blue; HCS CellMask, white) at 24 hpi. Scale bar, 20 μm.

(G) Co-infection with CTL2-R, but not CTL2-M923, protects HeLa cells from CTL2-M007-induced cell death. Infected cells (10 IFU/cell per strain) were monitored by live cell imaging from 12 to 40 hpi. At least 235 cells were analyzed per group.

Results shown represent mean ± SD (n = 3, one-way ANOVA + Newman-Keuls). See also Figure S2, Tables S1–S3, and Movies S4 and S5.

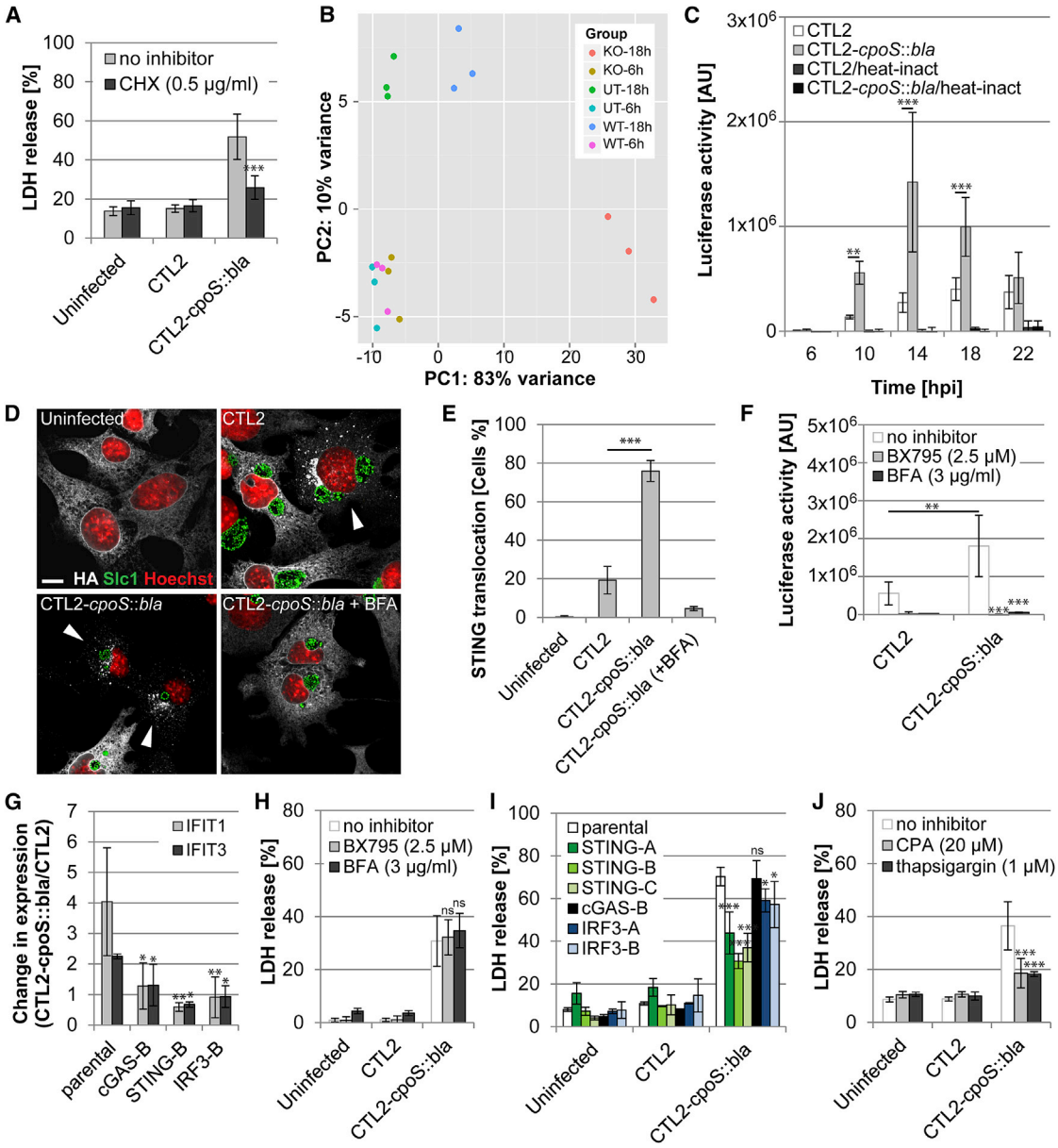

Figure 3. STING Mediates Type I IFN and Cell Death Responses to *cpoS* Mutants

(A) Cycloheximide (CHX; added 1 hr before infection) blocks CTL2-*cpoS*::*bla*-induced cell death in A2EN cells (10 IFU/cell, 24 hpi).

(B) Principal component analysis displaying differences between the transcriptional responses of uninfected A2EN cells (UT) and cells infected with CTL2 (WT) or CTL2-*cpoS*::*bla* (KO) (20 IFU/cell).

(C) Time course of luciferase activity in A2EN-ISRE reporter cells infected with the indicated strains (10 IFU/cell). Heat-inactivated (56°C, 30 min) bacteria served as control.

(D and E) Morphological (D) and quantitative (E) assessment of STING translocation in response to infection with CTL2 *cpoS::bla* at 18 hpi (10 IFU/cell) in *Gt* MLFs (expressing HA-tagged STING) by immunofluorescence microscopy (HA-tag, white; Slc1, green; Hoechst, red; confocal images; scale bar, 10 µm). BFA (3 µg/ml, added at 6 hpi) was included as a control. Arrowheads in (D) indicate cells with evidence of STING translocation.

(F) BX795 and BFA (added at 6 hpi) inhibit type I IFN responses induced by CTL2-*cpoS*::*bla* (20 IFU/cell). Luciferase activity in A2EN-ISRE cells was measured at 14 hpi.

(G) Induction of augmented ISG (IFIT1, IFIT3) expression in HeLa cells at 14 hpi (10 IFU/cell) is dependent on STING, cGAS, and IRF3.

(H) BX795 and BFA (added at 6 hpi) fail to inhibit CTL2-*cpoS*::*bla*-induced cell death in A2EN cells (20 IFU/cell, 24 hpi).

(I) HeLa cells deficient for STING, but not IRF3 or cGAS, are partially protected from CTL2-*cpoS*::*bla*-induced cell death (10 IFU/cell, 24 hpi).

(J) SERCA inhibitors (added 1 hr before infection) block CTL2-*cpoS*::*bla*-induced cell death in A2EN cells (10 IFU/cell, 24 hpi).

All experiments were conducted with purified EBs. If not stated otherwise, results shown represent mean ± SD (n = 3, one- or two-way ANOVA + Newman-Keuls or Sidak). See also Figures S3 and S4 and Table S4.

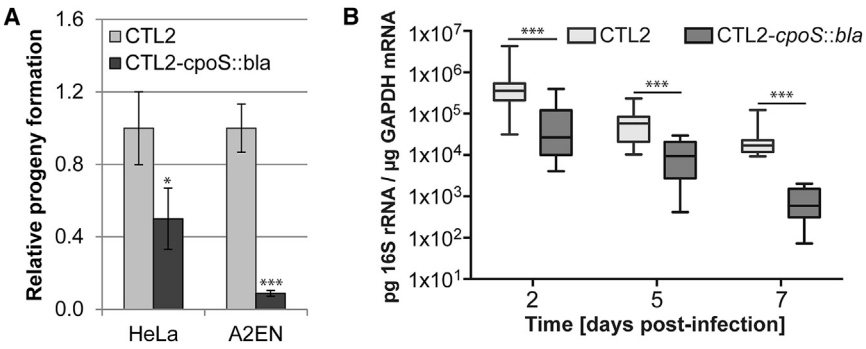

Figure 4. *cpoS* Mutants Are Defective for Propagation in Cell Culture and in Mice

(A) CTL2 *cpoS::bla* produces less-infectious progeny. The number of infectious bacteria was quantified at 34 hpi, normalized to the input, and displayed relative to progeny produced by CTL2 (mean ± SD, n = 3, Student's t test).

(B) CpoS-deficient bacteria are cleared faster from the mouse genital tract (box-and-whisker plot, n = 13 (days 2 + 5), n = 8 (day 7), Mann-Whitney U test).

All experiments were conducted with density gradient purified EBs. See also Figure S4.

expressing luciferase under control of the IFN stimulated response element (ISRE), even at time points that precede the onset of cell death (i.e., 10 hpi) (Figure 3C).

STING Mediates IFN and Cell Death Responses to *cpoS* Mutants

Induction of type I IFN during infection with *Chlamydia* requires the ER protein STING that is activated by cyclic dinucleotides produced by the bacteria or by the DNA senor cGAS (Barker et al., 2013; Prantner et al., 2010). Activated STING re-localizes to perinuclear vesicles to initiate TBK1 kinase-dependent phosphorylation of the transcription factor IRF3 and expression of type I interferons (Ishikawa et al., 2009; Tanaka and Chen, 2012). The frequency of cells displaying STING translocation was 3-fold higher during infection with the CpoS mutant (Figures 3D and 3E), and this translocation was blocked by brefeldin A (BFA), an inhibitor of ER to Golgi protein transport (Figures 3D and 3E). Activation of the ISRE-luciferase reporter was blocked by both BFA and BX795, an inhibitor of TBK1 (Figure 3F). The augmented induction of ISG expression during infection with the CpoS mutant was abrogated in HeLa cells deficient for cGAS, STING, or IRF3 (Figures 3G and S4E), confirming that the exacerbated IFN response induced in the absence of CpoS requires the canonical STING-dependent signaling pathway.

We expected that perturbation of interferon signaling would block the death induced by *cpoS* mutants. Unexpectedly, BFA and BX795 as well as cGAS and IRF3 gene deletions failed to inhibit cell death (Figures 3H and 3I), suggesting that cell death and IFN responses to CpoS-deficient *Chlamydia* are uncoupled. However, STING-deficient HeLa cells were partially protected from cell death (Figure 3I). A similar rescue was observed in A2EN cells in which STING was depleted by shRNA-mediated gene silencing (Figures S4F and S4G) and in *Goldenticket* (*Gt*) MLFs, which have a defective allele of the STING gene (Figure S4H). Because STING interacts with the ER calcium pump SERCA2 (Lee et al., 2013) and calcium is a regulator of cell death (Orrenius et al., 2015), we next tested the effect of compounds that alter intracellular calcium homeostasis on the cell death induced by *cpoS* mutants. We observed that low concentrations of thapsigargin and cyclopiazonic acid (CPA), two inhibitors of SERCA activity, both reduced the cytotoxicity of CpoS-deficient *Chlamydia* (Figure 3J), providing a possible explanation for how STING mediates *Chlamydia*-induced cell death independent of its role in regulating interferon responses.

cpoS Mutants Are Cleared Faster from the Murine Genital Tract

We predicted that the net effect of increased cell death and exacerbated cytokine responses in the absence of CpoS would disrupt the infectious cycle. Indeed, while primary inclusion formation was indistinguishable between CTL2 and CTL2-*cpoS::bla* (Figure S4I), *cpoS* mutants were impaired in their ability to form infectious EBs in both HeLa and A2EN cells (Figure 4A). When we challenged female mice transcervically, bacterial loads for the CpoS-deficient strain declined significantly faster between day 2 and day 7 post-infection (Figure 4B). Expression levels of TNF-α and GBP2 (an ISG) mirrored this trend (Figures S4J and S4K). These results demonstrate that CpoS is a virulence factor that is required for optimal infection of animals.

DISCUSSION

Our study demonstrates that *C. trachomatis* actively counteracts cell death-inducing signals initiated within infected cells in response to inclusions. Inactivation of a single Inc protein was sufficient to cause the early death of the majority of cells (Figure 2B). The observed heterogeneity in cell fate among infected cells (Figures 1 and S1) suggests the induction of multiple pro-death signals but could also reflect the crosstalk between signaling pathways (Vanden Berghe et al., 2015). Indeed, inhibition of any one specific death pathway often alters the mode and kinetics of cell death instead of conferring complete protection (Galluzzi et al., 2012). It is possible that our inability to block cell death by inhibiting individual pathways (Figure S3) reflects this inherent complexity. Because the protection conferred by CpoS is restricted to the inclusion in which it resides (Figure 2G), we consider it unlikely that this Inc is responsible for the ability of *C. trachomatis* to enhance resistance of infected cells to extrinsic inducers of apoptosis (Sharma and Rudel, 2009).

Chlamydia-infected cells produce TNF-α and type I IFNs (Finethy and Coers, 2016), which can induce cell death or enhance the susceptibility of cells to pro-death stimuli (Malireddi and Kanneganti, 2013; Van Herreweghe et al., 2010). Yet, given that uninfected cells adjacent to cells infected with *cpoS* mutants were not especially prone to death (Figure 1F), it is unlikely that the enhanced cytotoxicity was caused by enhanced induction of these cytokines. Furthermore, inhibition of TBK1 and genetic inactivation of IRF3 blocked the IFN response, but not cell death (Figure 3), indicating that cell death is not linked to either cytokines or IRF3-dependent cell death pathways described in other

systems (Di Paolo et al., 2013). Nevertheless, the enhanced cytokine responses imply that host cells are sensitized to the presence of CpoS-deficient inclusions and indicate that one of the functions of CpoS is to counteract cell-autonomous defense programs by masking the presence of bacterial signals from host cells.

For some vacuolar pathogens, the loss of niche integrity can trigger host cell death (Fredlund and Enninga, 2014). It is possible that CpoS preserves host cell viability by conferring stability to the inclusion. In *Salmonella typhimurium* and *Legionella pneumophila,* the effectors SifA or SdhA, respectively, counteract the action of secreted phospholipases that otherwise would compromise the integrity of the vacuole (Creasey and Isberg, 2012; Ruiz-Albert et al., 2002). Enhanced release of *L. pneumophila* factors from damaged vacuoles triggers type I IFN responses and cell death in macrophages (Creasey and Isberg, 2012). We consider this unlikely in our system because time-lapse microscopy of infected cells indicated that in cells undergoing necrosis the collapse of the Cpos-deficient inclusion membrane occurred either simultaneously with the rupture of the host cell membrane or only shortly before. Moreover, in cells undergoing apoptosis, inclusion integrity was preserved throughout the membrane blebbing stage (Movie S3).

Because CpoS interacts with host Rab GTPases (Mirrashidi et al., 2015; Rzomp et al., 2006) (Figures 2C and 2D; Table S3), and inhibition of vesicular transport blocks STING translocation (Figures 3D and 3E), we predict that CpoS suppresses IFN responses by interfering with membrane-trafficking events. An analogous strategy is used by *Shigella flexneri* to inhibit ER to ERGIC trafficking and STING signaling by targeting ARF GTPases (Dobbs et al., 2015). The specific roles of the many CpoS-interacting Rab and Inc proteins in restricting STING translocation and IFN induction remain to be determined, yet we predict that there are also non-vesicular traffic-dependent activities regulated by CpoS, since the contribution of STING to cell death was independent of its exit from the ER (Figure 3H). STING localizes to ER-mitochondria contact sites (Marchi et al., 2014) and interacts with the ER calcium pump SERCA (Lee et al., 2013). Our observation that low doses of SERCA inhibitors, which deplete calcium pools in the ER (Birkett et al., 1999), partially blocked the cell death induced by *cpoS* mutants (Figure 3J) suggests that STING may be a regulator of calcium-mediated cell death.

In conclusion, we provide evidence that *C. trachomatis* relies on CpoS to dampen the activation of cytokine and cell death pathways that control *Chlamydia* growth. We predict that analysis of Inc-dependent activities will reveal novel immune detection and cell protection pathways and highlight host signaling events that can be targeted to ameliorate *Chlamydia*-induced pathologies.

EXPERIMENTAL PROCEDURES

A full description of the procedures can be found in Supplemental Experimental Procedures.

Cell Culture and Infection

HeLa (ATCC CCL-2), Vero (ATCC CCL-81), HEK293T (ATCC CRL-3216), A2EN (Buckner et al., 2011), and THP-1 (ATCC TIB-202) cells; *Gt* MLFs (Barker et al., 2013); and C57BL/6 MLFs (Jorgensen et al., 2011) were maintained under standard cell culture conditions. Lentiviruses were used to generate stable silencing of STING in A2EN cells (shRNA-based) and for gene editing in HeLa cells (CRISPR/Cas9 system). *C. trachomatis* strain L2/434/Bu (CTL2; ATCC VR-902B), the rifampin-resistant variant CTL2-R (Nguyen and Valdivia, 2012) and derivatives described in this study were propagated in Vero cells. When indicated, infections were conducted with density gradient purified EBs (Saka et al., 2011). Cells treated with bacteria were centrifuged (1,500 × g, 30 min) to enhance infection. To quantify infectious progeny formation, bacteria were harvested from infected cell monolayers at 34 hpi and used to infect fresh cell monolayers.

Generation of Genetically Modified *Chlamydia* Strains

CTL2-M007 and CTL2-M923 (Kokes et al., 2015) were sequenced as described previously (Snavely et al., 2014). *Chlamydia* recombinants were generated by lateral gene transfer and genotyped as described previously (Nguyen and Valdivia, 2012). To enable complementation, expression of fluorescent proteins, or genetic disruption of CTL0481, *Chlamydia* were transformed (Wang et al., 2011) with derivatives of the *E. coli-Chlamydia* shuttle vector p2TK2-SW2 (Agaisse and Derré, 2013) or the TargeTron vector pDFTT3 (Johnson and Fisher, 2013).

Cell Death Analysis and Luciferase Reporter Assay

For the analysis of live cells, imaging was performed with a Zeiss Axio Observer.Z1 microscope. Membrane integrity was assessed by addition of propidium iodide. Active caspase-3 was detected in live cells by incubation with NucView 488 caspase-3 substrate (Biotium) or by immunofluorescence staining with anti-active caspase-3 antibodies (BD Pharmingen). Host cell lysis and DEVD cleavage were measured using the in vitro cytotoxicity kit (Sigma-Aldrich) and the fluorimetric caspase-3 assay kit (Sigma-Aldrich), respectively. The activation of IFN-dependent genes was assessed using an A2EN-ISRE-luciferase reporter cell line generated with the Cignal Lenti ISRE Reporter (Luc) Kit (QIAGEN).

Immunodetection Assays

Protein extracts were generated by lysing cells in boiling 1% SDS buffer, resolved by SDS-PAGE, and transferred to nitrocellulose membranes (Bio-Rad). Primary rabbit antibodies used included anti-CpoS, anti-OmpA (K. Fields, University of Kentucky), anti-FLAG (Sigma-Aldrich, F7425), anti-STING (Cell Signaling, 13647S), anti-cGAS (Cell Signaling, 15102S), and anti-IRF3 (Cell Signaling, 4302S). Primary mouse antibodies include anti-β-actin (Sigma-Aldrich, A2228). Fluorescently labeled secondary antibodies (LI-COR Biosciences) were used, and signals were recorded with an Odyssey Fc imaging system (LI-COR Biosciences). For immunofluorescence staining, primary antibodies included rabbit-anti-Slc1 (Chen et al., 2014) and anti-active-caspase-3 (BD Pharmingen, 559565), mouse-anti-OmpA (M. Scidmore, Cornell University), rabbit-anti-CT229 (T. Hackstadt, RML/NIAID), and rat-anti-HA (Sigma-Aldrich 11867423001). DNA and cells were stained with Hoechst 33258 (Life Technologies) and HCS CellMask Deep Red stain (Life Technologies), respectively. Images were acquired on a Zeiss Observer.Z1 epifluorescence microscope or a Zeiss 780 inverted confocal microscope.

Identification of CpoS-Interacting Proteins

Lysates from cells infected with CTL2-M007 expressing CpoS-FLAG or untagged CpoS were incubated with ANTI-FLAG M2 magnetic beads (Sigma-Aldrich). After immunoprecipitation, bound proteins were eluted and separated by SDS-PAGE. LC-MS/MS was used to identify proteins enriched in samples from cells infected with CpoS-FLAG expressing bacteria. For validation, HeLa cells were transfected with a Rab1A-EGFP expression plasmid (Rzomp et al., 2003).

Murine Infection Model

Female C57BL/6 mice (Jackson Laboratory) were treated with 2.5 mg medroxyprogesterone subcutaneously. Seven days later, mice were infected transcervically with 1×10^7 EBs per mouse (Coers et al., 2011). Mice were sacrificed, and upper genital tract samples were immediately homogenized. RNA was isolated by TRIzol (Thermo Fisher Scientific) extraction.

RNA-Seq and RT-qPCR

Total RNA was isolated using the RNeasy Mini Plus kit (QIAGEN). Sequencing libraries, prepared using the Kapa Stranded mRNA-Seq kit (Kapa Biosystems), were pooled and sequenced together on a total of three lanes of Illumina HiSeq 2000/2500 to obtain 50 bp single-end reads that were processed, mapped, and counted. Normalization and differential expression analysis were carried out using the DESeq2 R package (Love et al., 2014). A cutoff false discovery rate (FDR) of less than 0.001 and a log fold change of more than 1 were used to select significantly differentially expressed genes. RT-qPCR was conducted using the Power SYBR Green RNA-to-CT 1-Step Kit (Thermo Fisher Scientific). PCR targets and primers are listed in Supplemental Experimental Procedures.

Statistics

If not stated otherwise, statistical analysis was performed using the software GraphPad Prism 6.01 (*$p < 0.05$; **$p < 0.01$; ***$p < 0.001$; ns, not significant).

SUPPLEMENTAL INFORMATION

Supplemental Information includes four figures, four tables, five movies, and Supplemental Experimental Procedures and can be found with this article at http://dx.doi.org/10.1016/j.chom.2016.12.002.

AUTHOR CONTRIBUTIONS

Conceptualization, B.S.S. and R.H.V.; Investigation, B.S.S., R.J.B., R.F., and R.M.B.; Writing – Original Draft, B.S.S. and R.H.V.; Resources, V.K.C.; Supervision, G.K., J.C., and R.H.V.

ACKNOWLEDGMENTS

We thank the Duke University Core facilities for their technical support and T. Hackstadt (RML/NIAID), M. Scidmore (Cornell University), K. Fields (University of Kentucky), I. Dérre (University of Virginia), H.A. Saka (National University of Cordoba), D.J. Fisher (Southern Illinois University), and K. Spaeth for sharing cell lines, plasmids, and reagents. This work was supported by the European Union's Seventh Framework Program (grant agreement PIOF-GA-2013-626116), the National Institutes of Health (NIH) (R01AI100759 and R01AI103197), a Burroughs Wellcome Fund PATH Award, and a National Science Foundation (NSF) predoctoral award.

Received: September 16, 2016
Revised: November 3, 2016
Accepted: December 7, 2016
Published: December 29, 2016

REFERENCES

Agaisse, H., and Derré, I. (2013). A *C. trachomatis* cloning vector and the generation of *C. trachomatis* strains expressing fluorescent proteins under the control of a *C. trachomatis* promoter. PLoS ONE *8*, e57090.

Bannantine, J.P., Griffiths, R.S., Viratyosin, W., Brown, W.J., and Rockey, D.D. (2000). A secondary structure motif predictive of protein localization to the chlamydial inclusion membrane. Cell. Microbiol. *2*, 35–47.

Barker, J.R., Koestler, B.J., Carpenter, V.K., Burdette, D.L., Waters, C.M., Vance, R.E., and Valdivia, R.H. (2013). STING-dependent recognition of cyclic di-AMP mediates type I interferon responses during *Chlamydia trachomatis* infection. MBio *4*, e00018–e13.

Birkett, S.D., Jeremy, J.Y., Watts, S.M., Shukla, N., Angelini, G.D., and McArdle, C.A. (1999). Inhibition of intracellular Ca2+ mobilisation by low antiproliferative concentrations of thapsigargin in human vascular smooth-muscle cells. J. Cardiovasc. Pharmacol. *33*, 204–211.

Buckner, L.R., Schust, D.J., Ding, J., Nagamatsu, T., Beatty, W., Chang, T.L., Greene, S.J., Lewis, M.E., Ruiz, B., Holman, S.L., et al. (2011). Innate immune mediator profiles and their regulation in a novel polarized immortalized epithelial cell model derived from human endocervix. J. Reprod. Immunol. *92*, 8–20.

Chen, Y.S., Bastidas, R.J., Saka, H.A., Carpenter, V.K., Richards, K.L., Plano, G.V., and Valdivia, R.H. (2014). The *Chlamydia trachomatis* type III secretion chaperone Slc1 engages multiple early effectors, including TepP, a tyrosine-phosphorylated protein required for the recruitment of CrkI-II to nascent inclusions and innate immune signaling. PLoS Pathog. *10*, e1003954.

Coers, J., Gondek, D.C., Olive, A.J., Rohlfing, A., Taylor, G.A., and Starnbach, M.N. (2011). Compensatory T cell responses in IRG-deficient mice prevent sustained *Chlamydia trachomatis* infections. PLoS Pathog. *7*, e1001346.

Creasey, E.A., and Isberg, R.R. (2012). The protein SdhA maintains the integrity of the *Legionella*-containing vacuole. Proc. Natl. Acad. Sci. USA *109*, 3481–3486.

Di Paolo, N.C., Doronin, K., Baldwin, L.K., Papayannopoulou, T., and Shayakhmetov, D.M. (2013). The transcription factor IRF3 triggers "defensive suicide" necrosis in response to viral and bacterial pathogens. Cell Rep. *3*, 1840–1846.

Dobbs, N., Burnaevskiy, N., Chen, D., Gonugunta, V.K., Alto, N.M., and Yan, N. (2015). STING activation by translocation from the ER is associated with infection and autoinflammatory disease. Cell Host Microbe *18*, 157–168.

Finethy, R., and Coers, J. (2016). Sensing the enemy, containing the threat: cell-autonomous immunity to *Chlamydia trachomatis*. FEMS Microbiol. Rev. fuw027.

Fredlund, J., and Enninga, J. (2014). Cytoplasmic access by intracellular bacterial pathogens. Trends Microbiol. *22*, 128–137.

Galluzzi, L., Vitale, I., Abrams, J.M., Alnemri, E.S., Baehrecke, E.H., Blagosklonny, M.V., Dawson, T.M., Dawson, V.L., El-Deiry, W.S., Fulda, S., et al. (2012). Molecular definitions of cell death subroutines: recommendations of the Nomenclature Committee on Cell Death 2012. Cell Death Differ. *19*, 107–120.

Gauliard, E., Ouellette, S.P., Rueden, K.J., and Ladant, D. (2015). Characterization of interactions between inclusion membrane proteins from *Chlamydia trachomatis*. Front. Cell. Infect. Microbiol. *5*, 13.

Hackstadt, T., Scidmore-Carlson, M.A., Shaw, E.I., and Fischer, E.R. (1999). The *Chlamydia trachomatis* IncA protein is required for homotypic vesicle fusion. Cell. Microbiol. *1*, 119–130.

Huang, W., Sherman, B.T., and Lempicki, R.A. (2009). Systematic and integrative analysis of large gene lists using DAVID bioinformatics resources. Nat. Protoc. *4*, 44–57.

Hutagalung, A.H., and Novick, P.J. (2011). Role of Rab GTPases in membrane traffic and cell physiology. Physiol. Rev. *91*, 119–149.

Ishikawa, H., Ma, Z., and Barber, G.N. (2009). STING regulates intracellular DNA-mediated, type I interferon-dependent innate immunity. Nature *461*, 788–792.

Johnson, C.M., and Fisher, D.J. (2013). Site-specific, insertional inactivation of incA in *Chlamydia trachomatis* using a group II intron. PLoS ONE *8*, e83989.

Jorgensen, I., Bednar, M.M., Amin, V., Davis, B.K., Ting, J.P., McCafferty, D.G., and Valdivia, R.H. (2011). The *Chlamydia* protease CPAF regulates host and bacterial proteins to maintain pathogen vacuole integrity and promote virulence. Cell Host Microbe *10*, 21–32.

Kokes, M., Dunn, J.D., Granek, J.A., Nguyen, B.D., Barker, J.R., Valdivia, R.H., and Bastidas, R.J. (2015). Integrating chemical mutagenesis and whole-genome sequencing as a platform for forward and reverse genetic analysis of *Chlamydia*. Cell Host Microbe *17*, 716–725.

Labbé, K., and Saleh, M. (2008). Cell death in the host response to infection. Cell Death Differ. *15*, 1339–1349.

Lee, M.N., Roy, M., Ong, S.E., Mertins, P., Villani, A.C., Li, W., Dotiwala, F., Sen, J., Doench, J.G., Orzalli, M.H., et al. (2013). Identification of regulators of the innate immune response to cytosolic DNA and retroviral infection by an integrative approach. Nat. Immunol. *14*, 179–185.

Love, M.I., Huber, W., and Anders, S. (2014). Moderated estimation of fold change and dispersion for RNA-seq data with DESeq2. Genome Biol. *15*, 550.

Malireddi, R.K., and Kanneganti, T.D. (2013). Role of type I interferons in inflammasome activation, cell death, and disease during microbial infection. Front. Cell. Infect. Microbiol. *3*, 77.

Marchi, S., Patergnani, S., and Pinton, P. (2014). The endoplasmic reticulum-mitochondria connection: one touch, multiple functions. Biochim. Biophys. Acta *1837*, 461–469.

Mi, H., Poudel, S., Muruganujan, A., Casagrande, J.T., and Thomas, P.D. (2016). PANTHER version 10: expanded protein families and functions, and analysis tools. Nucleic Acids Res. *44* (D1), D336–D342.

Mirrashidi, K.M., Elwell, C.A., Verschueren, E., Johnson, J.R., Frando, A., Von Dollen, J., Rosenberg, O., Gulbahce, N., Jang, G., Johnson, T., et al. (2015). Global mapping of the Inc-human interactome reveals that retromer restricts *Chlamydia* infection. Cell Host Microbe *18*, 109–121.

Mylonas, I. (2012). Female genital *Chlamydia trachomatis* infection: where are we heading? Arch. Gynecol. Obstet. *285*, 1271–1285.

Nguyen, B.D., and Valdivia, R.H. (2012). Virulence determinants in the obligate intracellular pathogen *Chlamydia trachomatis* revealed by forward genetic approaches. Proc. Natl. Acad. Sci. USA *109*, 1263–1268.

Orrenius, S., Gogvadze, V., and Zhivotovsky, B. (2015). Calcium and mitochondria in the regulation of cell death. Biochem. Biophys. Res. Commun. *460*, 72–81.

Prantner, D., Darville, T., and Nagarajan, U.M. (2010). Stimulator of IFN gene is critical for induction of IFN-beta during *Chlamydia muridarum* infection. J. Immunol. *184*, 2551–2560.

Randow, F., MacMicking, J.D., and James, L.C. (2013). Cellular self-defense: how cell-autonomous immunity protects against pathogens. Science *340*, 701–706.

Rockey, D.D., Scidmore, M.A., Bannantine, J.P., and Brown, W.J. (2002). Proteins in the chlamydial inclusion membrane. Microbes Infect. *4*, 333–340.

Ruiz-Albert, J., Yu, X.J., Beuzón, C.R., Blakey, A.N., Galyov, E.E., and Holden, D.W. (2002). Complementary activities of SseJ and SifA regulate dynamics of the *Salmonella typhimurium* vacuolar membrane. Mol. Microbiol. *44*, 645–661.

Rzomp, K.A., Scholtes, L.D., Briggs, B.J., Whittaker, G.R., and Scidmore, M.A. (2003). Rab GTPases are recruited to chlamydial inclusions in both a species-dependent and species-independent manner. Infect. Immun. *71*, 5855–5870.

Rzomp, K.A., Moorhead, A.R., and Scidmore, M.A. (2006). The GTPase Rab4 interacts with *Chlamydia trachomatis* inclusion membrane protein CT229. Infect. Immun. *74*, 5362–5373.

Saka, H.A., Thompson, J.W., Chen, Y.S., Kumar, Y., Dubois, L.G., Moseley, M.A., and Valdivia, R.H. (2011). Quantitative proteomics reveals metabolic and pathogenic properties of *Chlamydia trachomatis* developmental forms. Mol. Microbiol. *82*, 1185–1203.

Sharma, M., and Rudel, T. (2009). Apoptosis resistance in *Chlamydia*-infected cells: a fate worse than death? FEMS Immunol. Med. Microbiol. *55*, 154–161.

Snavely, E.A., Kokes, M., Dunn, J.D., Saka, H.A., Nguyen, B.D., Bastidas, R.J., McCafferty, D.G., and Valdivia, R.H. (2014). Reassessing the role of the secreted protease CPAF in *Chlamydia trachomatis* infection through genetic approaches. Pathog. Dis. *71*, 336–351.

Tanaka, Y., and Chen, Z.J. (2012). STING specifies IRF3 phosphorylation by TBK1 in the cytosolic DNA signaling pathway. Sci. Signal. *5*, ra20.

Van Herreweghe, F., Festjens, N., Declercq, W., and Vandenabeele, P. (2010). Tumor necrosis factor-mediated cell death: to break or to burst, that's the question. Cell. Mol. Life Sci. *67*, 1567–1579.

Vanden Berghe, T., Kaiser, W.J., Bertrand, M.J., and Vandenabeele, P. (2015). Molecular crosstalk between apoptosis, necroptosis, and survival signaling. Mol. Cell. Oncol. *2*, e975093.

Wang, Y., Kahane, S., Cutcliffe, L.T., Skilton, R.J., Lambden, P.R., and Clarke, I.N. (2011). Development of a transformation system for *Chlamydia trachomatis*: restoration of glycogen biosynthesis by acquisition of a plasmid shuttle vector. PLoS Pathog. *7*, e1002258.

Ward, M.E. (1988). The chlamydial developmental cycle. In Micobiology of *Chlamydia*, A.L. Barron, ed. (Boca Raton, FL: CRC Press), pp. 71–95.